Progress In Electromagnetics Research Letters, Vol. 32, 109–118, 2012

DISTORTION ANALYSIS OF ELECTROMAGNETIC FIELD SENSORS IN LAGUERRE FUNCTIONS SUBSPACE

S. Saboktakin and B. Kordi*

Department of Electrical and Computer Engineering, University of Manitoba Winnipeg, MB R3T 5V6, Canada

Abstract—A time-domain approach for distortion analysis of electromagnetic field senors is developed in Laguerre functions subspace. Using Laguerre convolution preservation property, it is proved that every electromagnetic field sensor corresponds to an equivalent discrete-time LTI system. The equivalent discrete-time system is compared to a reference system as a measure of distortion. Further, this analysis may be performed repeatedly to obtain a bandwidth-limited distortion characteristic. The method is employed to compare the distortion characteristic of an asymptotic conical dipole (ACD) to wire monopoles of various lengths. A time-domain simulation is performed in order to find the distortion characteristics by solving an electric field integral equation (EFIE) using the method of moments (MoM).

1. INTRODUCTION

Electromagnetic field sensors are defined as passive devices which convert electromagnetic fields into an electric signal at their terminals [1]. D-dot sensors are a class of electric field sensors which deliver the time derivative of the incident electric field at their terminals. D-dot sensors have been used widely in a variety of measurement procedures such as high-voltage measurements [2], high-power electromagnetic measurements [3], lightning spectrum measurements [4], and partial discharge measurements [5].

To characterize the distortion behavior of an electromagnetic field sensor, such as a D-dot sensor, one can use time-domain techniques as noted in [6], where *fidelity* is introduced as a time-domain distortion characteristic. Fidelity inherently measures the

Received 8 May 2012, Accepted 1 June 2012, Scheduled 8 June 2012

* Corresponding author: Behzad Kordi (kordib@cc.umanitoba.ca).

similarity of the sensor response and the ideal response, however, it has some drawbacks. Fidelity should be calculated for every time-domain waveform which the sensor measures. As a waveform-dependent characteristic, calculation of fidelity is not a simple task when comparing two or more sensor receiving a variety of time-domain waveforms [7].

An alternative distortion measure for electromagnetic field sensors is investigated in a recent publication by the authors [8] based on Hermite-Gauss orthogonal functions. In this method, the sensor is considered as a linear operator and a transformation matrix is calculated for the system using Hermite-Gauss functions as the basis set. The matrix is compared to a reference matrix in order to determine the performance of the system. As the matrix describes the system for a subspace of waveforms, the obtained distortion measure is valid for a set of waveforms rather than a single waveform as it is the case using fidelity.

Study of linear systems in Laguerre subspaces has showed to be very advantageous as Laguerre functions properties aid to simplify the formulations [9]. In this paper, Laguerre orthogonal functions are used as the basis set in order to calculate the transformation matrix. We will show when Laguerre functions are employed as the basis functions, the transformation matrix is a special case of a Toeplitz matrix which in turn corresponds to a discrete-time linear time-invariant (LTI) system [10]. This makes the distortion analysis as simple as comparing the impulse response of the corresponding discrete-time system to an ideal discrete-time impulse response. A bandwidth-limited distortion analysis is performed in Laguerre subspace as the Laguerre functions of different orders have the same spectral content where the bandwidth is controlled by a scaling factor. As an application, distortion characteristic of an asymptotic conical dipole (ACD) [11], a commonly used D-dot sensor, is compared to that of wire monopoles of different lengths. Time-domain simulation of the ACD and the wire monopoles is performed by solving an electric field integral equation (EFIE) using the method of moments (MoM) [12].

2. LAGUERRE FUNCTIONS

Laguerre functions are defined as [13]

$$l_n^p(t) = (-1)^n \sqrt{2p} L_n(2pt) e^{-pt} \quad t \geq 0, \quad n = 0, 1, 2, \ldots \tag{1}$$

where p is a real positive scaling factor, and $L_n(t)$ is the nth order Laguerre polynomial [14]. Fig. 1 shows Laguerre functions for different orders assuming $p = 1$. Laguerre functions have many interesting properties including:

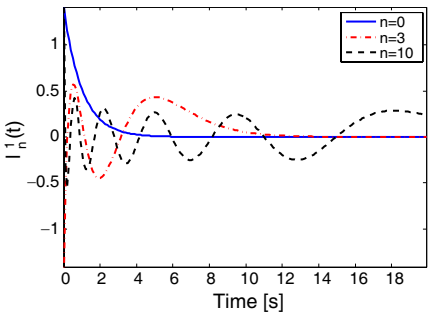

Figure 1. Different orders of Laguerre functions for $p = 1$.

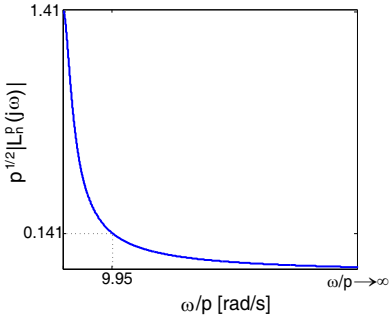

Figure 2. Variation of magnitude of the Fourier transform of Laguerre functions with respect to the frequency.

- Laguerre functions form an orthonormal basis set for $L^2(0,\infty)$ [15].
- The Fourier transform of $l_n^p(t)$, $L_n^p(j\omega)$, is given by [13]

$$L_n^p(j\omega) = \mathcal{F}[l_n^p(t)] = \sqrt{2p}\frac{e^{-j(2n+1)\tan^{-1}\left(\frac{\omega}{p}\right)}}{\sqrt{\omega^2+p^2}}. \tag{2}$$

From (2), one can see that the magnitude of the Fourier transform of Laguerre functions, $|L_n^p(j\omega)|$, is the same for any order of the function. Using (2), it is shown that the frequency at which $|L_n^p(j\omega)|$ falls to 10% of its maximum value (see Fig. 2) is given by

$$\frac{\omega_{10\%}}{p} \cong 9.95 \quad \text{or} \quad f_{10\%} \cong 1.58p. \tag{3}$$

- Convolution of Laguerre functions is written as a summation of Laguerre functions [13]

$$l_n^p(t) * l_m^p(t) = \frac{1}{\sqrt{2p}}\left[l_{n+m}^p(t) + l_{n+m+1}^p(t)\right]. \tag{4}$$

This is an extremely useful property which makes the transformation matrix a special case of a Toeplitz matrix.

3. DISTORTION ANALYSIS IN LAGUERRE FUNCTIONS SUBSPACE

The electromagnetic field sensor under study is considered as an LTI system as shown in Fig. 3(a), where, for example, the incident electric

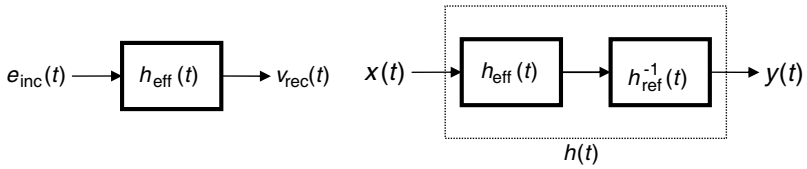

Figure 3. Block diagram of (a) the LTI system representation of an electric field sensor and, (b) an equivalent system consisting of the sensor and the reference sensor in cascade.

field and the received voltage at the terminals of the sensor are the input and the output of the LTI system, respectively. A distortion analysis is performed by comparing the sensor's characteristics to that of a reference sensor. Consider an equivalent system consisting of the sensor, $h_{\text{eff}}(t)$, cascaded with the inverse of the reference sensor, $h_{\text{ref}}^{-1}(t)$ (See Fig. 3(b)). The equivalent system has the impulse response given by

$$h(t) = h_{\text{eff}}(t) * h_{\text{ref}}^{-1}(t) \tag{5}$$

where $*$ denotes the convolution operator. For a D-dot sensor, for example, $h(t)$ is the impulse response of a cascaded ideal integrator (inverse of an ideal differentiator) and that of the D-dot sensor itself. The equivalent sensor as determined by (5) should be ideally compared with the identity system that has an impulse response of the Dirac delta function.

3.1. Calculation of the Transformation Matrix

Assume that the input signal to the equivalent system shown in Fig. 3(b) is $x(t)$ and the output is $y(t)$. Since we are measuring causal pulses with finite energies, both $x(t)$ and $y(t)$ belong to the subspace of quadratically integrable functions, $L^2(0,\infty)$. Therefore, a basis set consisting of Laguerre functions, $B = \{l_0^p(t), l_1^p(t), l_2^p(t), \ldots\}$, can be employed to represent $x(t)$ and $y(t)$ as

$$x(t) = \sum_{i=0}^{\infty} x_i l_i^p(t) \tag{6}$$

$$y(t) = \sum_{i=0}^{\infty} y_i l_i^p(t) \tag{7}$$

where $l_i^p(t)$ is defined as given by (1). The coefficients x_i and y_i, in (6) and (7), are given by

$$x_i = \langle x(t), l_i^p(t) \rangle \tag{8}$$

$$y_i = \langle y(t), l_i^p(t) \rangle \tag{9}$$

where $\langle ., . \rangle$ is the inner product operator. Eqs. (8), and (9) are obtained as a direct implication of the orthonrmality property of Laguerre functions. Assuming $\bar{x} = [x_0, x_1, x_2, \ldots]^t$ and $\bar{y} = [y_0, y_1, y_2, \ldots]^t$ are vector representations of $x(t)$ and $y(t)$ in Laguerre functions subsapace, then a transformation matrix, $\mathbf{L} = [l_{ij}]$ can be found which relates $\bar{x}$ and $\bar{y}$ vector representations as

$$\bar{y} = \mathbf{L}\,\bar{x}. \tag{10}$$

The ijth element of the transformation matrix, $\mathbf{L}$, is calculated as [8]

$$l_{ij} = \left\langle h(t) * l_{j-1}^p(t), l_{i-1}^p(t) \right\rangle \qquad i, j \geq 1. \tag{11}$$

Since the impulse response $h(t)$ is a causal time-domain signal with finite energy it can be expressed in terms of Laguerre basis functions as

$$h(t) = \sum_{k=0}^{\infty} h_k l_k^p(t). \tag{12}$$

Substituting (12) in (11) and exchanging the summation and the inner product results in

$$l_{ij} = \sum_{k=0}^{\infty} h_k \left\langle l_k^p(t) * l_{j-1}^p(t), l_{i-1}^p(t) \right\rangle. \tag{13}$$

Using Laguerre functions convolution property given in (4), (13) can be written as

$$l_{ij} = \frac{1}{\sqrt{2p}} \sum_{k=0}^{\infty} h_k \left\langle l_{k+j-1}^p(t), l_{i-1}^p(t) \right\rangle + \frac{1}{\sqrt{2p}} \sum_{k'=0}^{\infty} h_{k'} \left\langle l_{k'+j}^p(t), l_{i-1}^p(t) \right\rangle. \tag{14}$$

Due to orthonormality of Laguerre functions, (14) is simplified to

$$l_{ij} = \frac{1}{\sqrt{2p}} \sum_{k=0}^{\infty} h_k \delta\left[k + j - i\right] + \frac{1}{\sqrt{2p}} \sum_{k'=0}^{\infty} h_{k'} \delta\left[k' + j - i + 1\right] \tag{15}$$

where $\delta[n]$ is the discrete impulse function defined as

$$\delta[n] = \begin{cases} 1 & \text{if } n = 0 \\ 0 & \text{otherwise} \end{cases}. \tag{16}$$

Eq. (15) can be expressed in a more compact form as

$$l_{ij} = \frac{1}{\sqrt{2p}}(h_{i-j}u(i-j) + h_{i-j-1}u(i-j-1)) \tag{17}$$

where $u(.)$ is the unit step function. The following properties result from (17):

(i) The diagonal elements are all equal to each other and have the value of $\frac{1}{\sqrt{2p}}h_0$.

(ii) For $i < j$ both $u(i-j)$ and $u(i-j-1)$ are zero, i.e., the elements above the matrix diagonal are all zero.

(iii) The first column $\mathbf{L}_1$ has the form of

$$\mathbf{L}_1 = [h_0, h_0 + h_1, h_1 + h_2, \ldots, h_i + h_{i+1}, \ldots]^t . \tag{18}$$

(iv) Other columns in the transformation matrix are shifted versions of the first column, i.e., the jth column is written as

$$\mathbf{L}_j = [\underbrace{0, 0, \ldots, 0}_{j-1}, h_0, h_0 + h_1, h_1 + h_2, \ldots, h_i + h_{i+1}, \ldots]^t. \tag{19}$$

The transformation matrix calculated in Laguerre subspace is given by

$$[l_{ij}] = \frac{1}{\sqrt{2p}} \begin{bmatrix} h_0 & 0 & 0 & 0 & \cdots \\ h_0 + h_1 & h_0 & 0 & 0 & \cdots \\ h_1 + h_2 & h_0 + h_1 & h_0 & 0 & \cdots \\ h_2 + h_3 & h_1 + h_2 & h_0 + h_1 & h_0 & \cdots \\ \vdots & \vdots & \vdots & \vdots & \ddots \end{bmatrix} . \tag{20}$$

3.2. Equivalent Discrete-time LTI System

In [10], it is proved that the transformation matrix for every discrete-time LTI system with the impulse response $h_{eq}[n] = t_n$ is given by

$$[t_{ij}] = \begin{bmatrix} t_0 & 0 & 0 & 0 & \cdots \\ t_1 & t_0 & 0 & 0 & \cdots \\ t_2 & t_1 & t_0 & 0 & \cdots \\ t_3 & t_2 & t_1 & t_0 & \cdots \\ \vdots & \vdots & \vdots & \vdots & \ddots \end{bmatrix} \tag{21}$$

which is a special case of a Toeplitz matrix. Considering (19) and (20), we can observe that in Laguerre subspace, every continuous causal LTI system corresponds to a discrete time LTI system with the impulse response $h_{eq}[n]$ which is determined using

$$h_{eq}[n] = \begin{cases} \frac{1}{\sqrt{2p}}h_0 & \text{if } n = 0 \\ \frac{1}{\sqrt{2p}}(h_n + h_{n-1}) & \text{if } n \geq 1 \end{cases} . \tag{22}$$

Therefore, instead of comparing $h(t)$, as given in (5), with a Dirac delta function, we can compare $h_{eq}[n]$ with discrete impulse function as given by (16). The distance between normalized $h_{eq}[n]$ as a vector and the discrete impulse function is given by

$$d = \sqrt{\left(\hat{h}_0 - 1\right)^2 + \sum_{k=1}^{\infty}\left(\hat{h}_k + \hat{h}_{k-1}\right)^2} \tag{23}$$

where $[\hat{h}_0, \hat{h}_1, \hat{h}_2, \ldots]$ are the normalized coefficients of vector $[h_0, h_1, h_2, \ldots]$ to the energy of $h_{eq}[n]$. The value of d varies between 0 and $\sqrt{2}$ with smaller values corresponding to less distortion.

4. SIMULATION RESULTS

To demonstrate the application of the approach developed in this paper, a 5-cm ACD as well as 5, 10, and 15-cm wire monopoles are compared to an ideal D-dot senor. In this case, the equivalent system, as used in (5), is an ideal integrator cascaded by the sensor impulse response. To calculate the sensor impulse response, a time-domain simulation is performed. The sensors are modeled as wire structures. An electric field integral equation (EFIE) is solved to determine the current on each wire segment when the sensor is illuminated by a plane

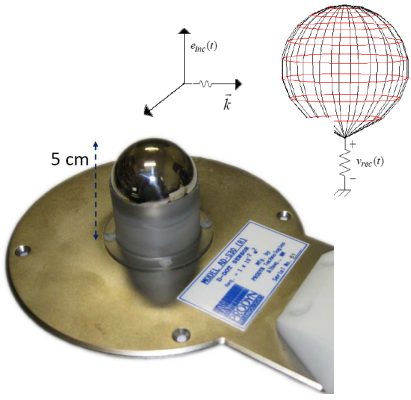

Figure 4. Photo of the ACD, simulated in this paper, and the wire model used for the simulations.

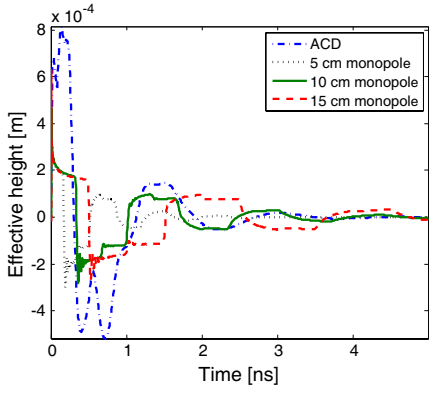

Figure 5. Calculated impulse responses for the ACD and the wire monopoles using time-domain simulations performed by solving an EFIE using the MoM.

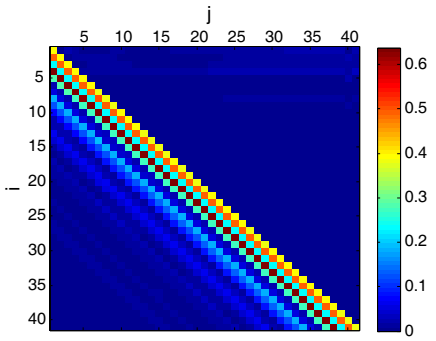

Figure 6. Calculated transformation matrix using Laguerre functions with $p = 10^{10}$ for a 5-cm ACD.

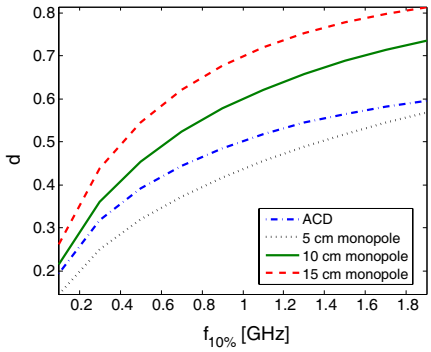

Figure 7. Calculated distortion measure, d, for the D-dot sensors for different frequency ranges.

wave [12]. A photo of the ACD simulated in this paper and its wire model are shown in Fig. 4.

The received voltage of every sensor, when exposed to a known incident electric field, is calculated. The transfer function for every sensor can be calculated in the frequency domain by dividing the Fourier transform of the received voltage to the Fourier transform of the incident electric field. Using an inverse Fourier transform, the time-domain impulse response, $h_{\text{eff}}(t)$, is determined. Fig. 5 shows the impulse responses calculated for the four sensors. Fig. 6 shows the calculated transformation matrix for an ACD using $p = 10^{10}$ as the scaling factor for Laguerre functions. As shown in Fig. 6, transformation matrix obtained using numerical simulations has the same structure as given in (20). Using the simulated data, d is calculated for the 4 sensors, for different values of p which correspond to different frequency ranges according to Fig. 2 and as given in (3). Fig. 7 shows the distortion characteristics of the four sensors as D-dot sensors where we have plotted d as defined in (23) for different values of p that correspond to different values of $f_{10\%}$. The 5-cm monopole is the best differentiator among the four, while the ACD comes in the second place. Although the 5-cm ACD has a higher level of distortion compared to a monopole of the same length, it has a higher sensitivity as observed in Fig. 5. Fig. 7 shows that the ACD has less distortion level when compared to 10 and 15-cm monopoles.

5. CONCLUSION

Distortion characteristics of an electromagnetic field sensor were studied by modeling the sensor as an LTI system. Using a Laguerre function expansion, a transformation matrix was calculated for the sensor/system. It was proved that by using Laguerre functions, the transformation matrix becomes a spacial case of a Toeplitz matrix that can be reduced to a vector. This matrix corresponds to a discrete-time LTI system. It was shown in this paper that by comparing this equivalent discrete-time LTI system to a reference discrete-time system, a quantitative measure of distortion is obtained. A spectral analysis is also possible using spectral properties of Laguerre functions. Finally, a 5-cm ACD along with 5, 10, and 15-cm monopoles are compared to an ideal D-dot sensor. It was concluded that the 5-cm monopole has the least distortion, but considering the sensitivity as a factor, the ACD is a more practical electric field D-dot sensor.

REFERENCES

1. "IEEE standard for calibration of electromagnetic field sensors and probes, excluding antennas, from 9 kHz to 40 GHz," IEEE Std 1309-2005 (Revision of IEEE Std 1309-1996), 2005.
2. Metwally, I. A., "D-dot probe for fast-front high-voltage measurement," *IEEE Trans. Instrumentation and Measurement*, Vol. 59, No. 8, 2211–2219, Aug. 2010.
3. Weber, T. and J. L. Ter Haseborg, "Measurement techniques for conducted HPEM signals," *IEEE Trans. Electromagnetic Compatibility*, Vol. 46, No. 3, 431–438, Aug. 2004.
4. Shumpert, T., M. Honnell, and G. Lott, "Measured spectral amplitude of lightning sferics in the HF, VHF, and UHF bands," *IEEE Trans. Electromagnetic Compatibility*, Vol. 24, No. 3, 368–369, 1982.
5. Sarathi, R. and G. Koperundevi, "UHF technique for identification of partial discharge in a composite insulation under ac and dc voltages," *IEEE Trans. Dielectrics and Electrical Insulation*, Vol. 15, No. 6, 1724–1730, Dec. 2008.
6. Lamensdorf, D. and L. Susman, "Baseband-pulse-antenna techniques," *IEEE Antennas and Propagation Magazine*, Vol. 36, 20–30, Feb. 1994.
7. Carro, P. and J. De Mingo, "Ultrawide-band antenna distortion characterization using Hermite-Gauss signal subspaces," *IEEE Antennas and Wireless Propagation Letters*, Vol. 7, 267–270, 2008.

8. Saboktakin, S. and B. Kordi, "Time-domain distortion analysis of wideband electromagnetic field sensors using Hermite-Gauss orthogonal functions," *IEEE Trans. Electromagnetic Compatibility*, 2011, doi:10.1109/TEMC.2011.2170997.
9. Kinoshita, Y. and O. Ohta, "Continuous-time system identification using compactly-supported filter kernels generated from Laguerre basis functions," *49th IEEE Conference on Decision and Control (CDC)*, 4461–4466, Dec. 2010.
10. Iohvidov, I. S., *Hankel and Toeplitz Matrices and Forms Algebraic Theory*, Birkhiuser, Boston, 1982.
11. Baum, C. E., "An equivalent-charge method for defining geometries of dipole antennas," *Sensor and Simulation Notes*, No. 72, 1969.
12. Miller, E. K., A. J. Poggio, and G. J. Burke, "An integro-differential equation technique for the time-domain analysis of thin wire structures," *Journal of Computational Physics*, Vol. 12, 24–48, 1973.
13. Budke, G., "On a convolution property characterizing the Laguerre functions," *Monatshefte für Mathematik*, Vol. 107, 281–285, 1989.
14. Szego, G., *Orthogonal Polynomials*, American Mathematical Society Providence, New York, 1939.
15. Loomis, L. H., "A short proof of the completeness of the Laguerre functions," *Bulletin of the American Mathematical Society*, Vol. 50, No. 6, 386–387, 1944.